

SUPPORTING INFORMATION

Title: Fabricating defogging metasurfaces via a water-based colloidal route

Author(s): Olena Khoruzhenko, Volodymyr Dudko, Sabine Rosenfeldt and Josef Breu*

Au NPs synthesis scheme

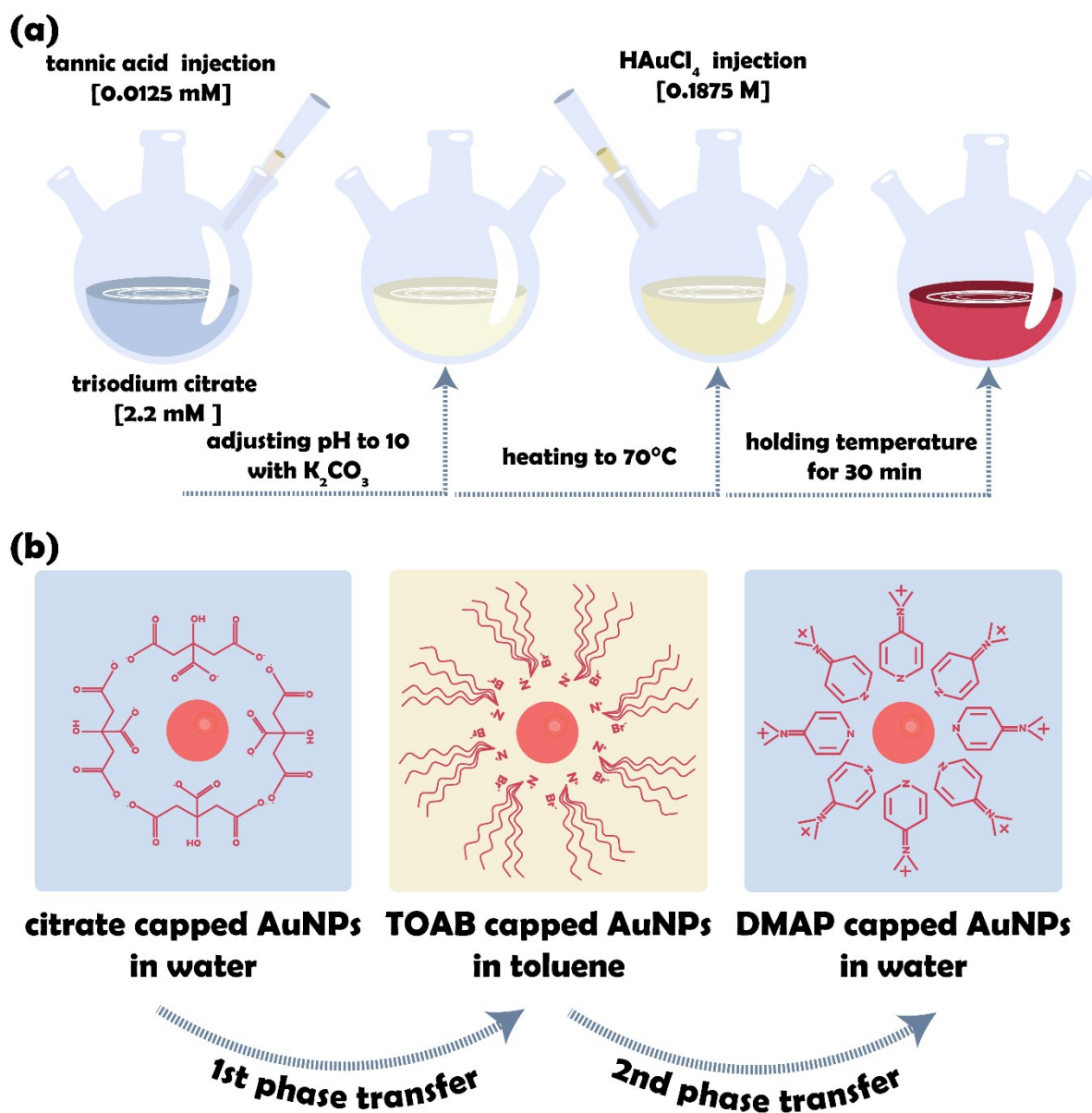


Figure S1. Scheme of Au NPs synthesis. **a** Step by step scheme of citrate capped Au NPs synthesis. **b** Two steps phase transfer of Au NPs into organic and back to aqueous phases DMAP capped Au NPs.

Size distribution and zeta potential measurements

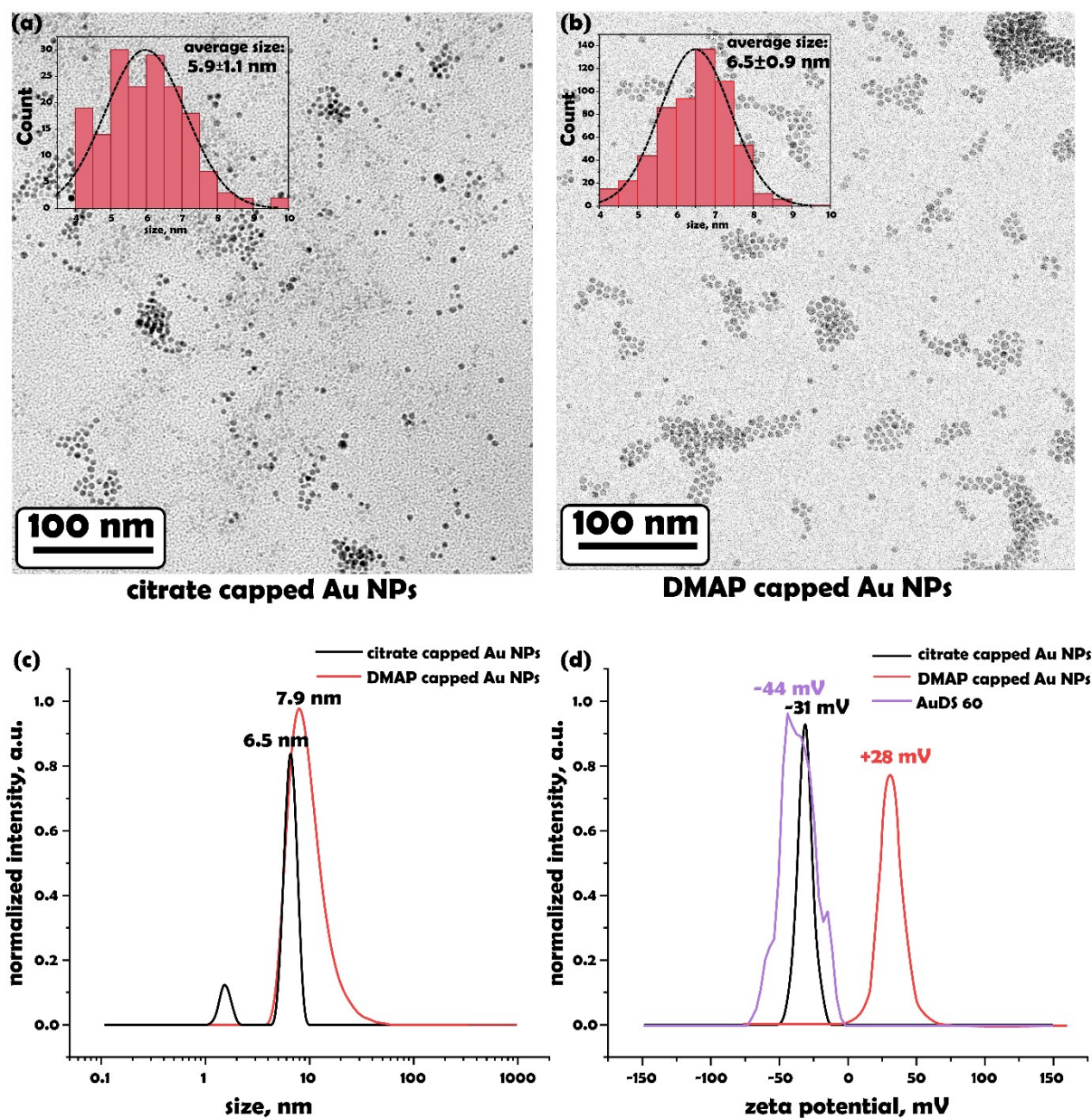


Figure S2. Size and charge characterization of nanomaterials. **a** TEM image of citrate capped Au NPs. Inserted histogram of the diameter distribution of 150 particles. **b** TEM image of DMAP capped AuNPs. Inserted histogram of the diameter distribution of 400 particles. **c** Hydrodynamic diameter according to DLS measurement. **d** Zeta potential for citrate capped Au NPs, for AuDS 60 at pH 7, and for DMAP capped Au NPs at pH 12.5.

UV-Vis spectra of Au NPs

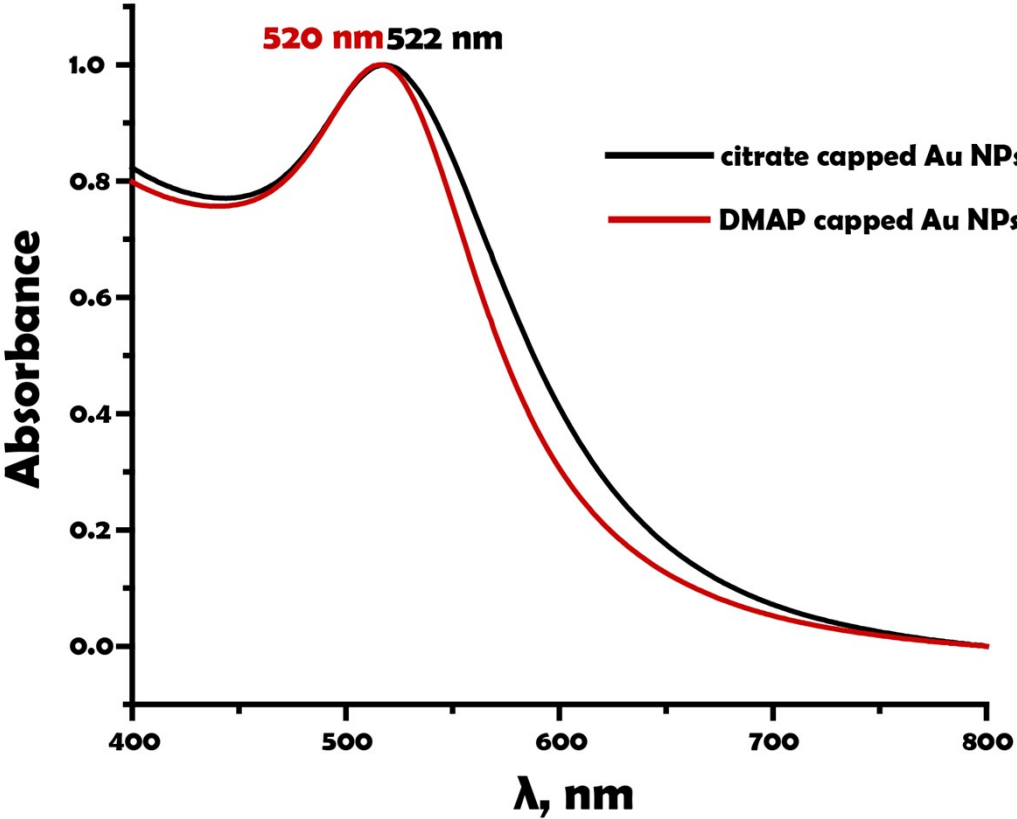


Figure S3. Characteristic UV-Vis spectra for aqueous suspensions of citrate and DMAP capped Au NPs and LSPR peaks positions.

XRD pattern of $\text{NH}_4^+/\text{Na}^+$ ordered heterostructures

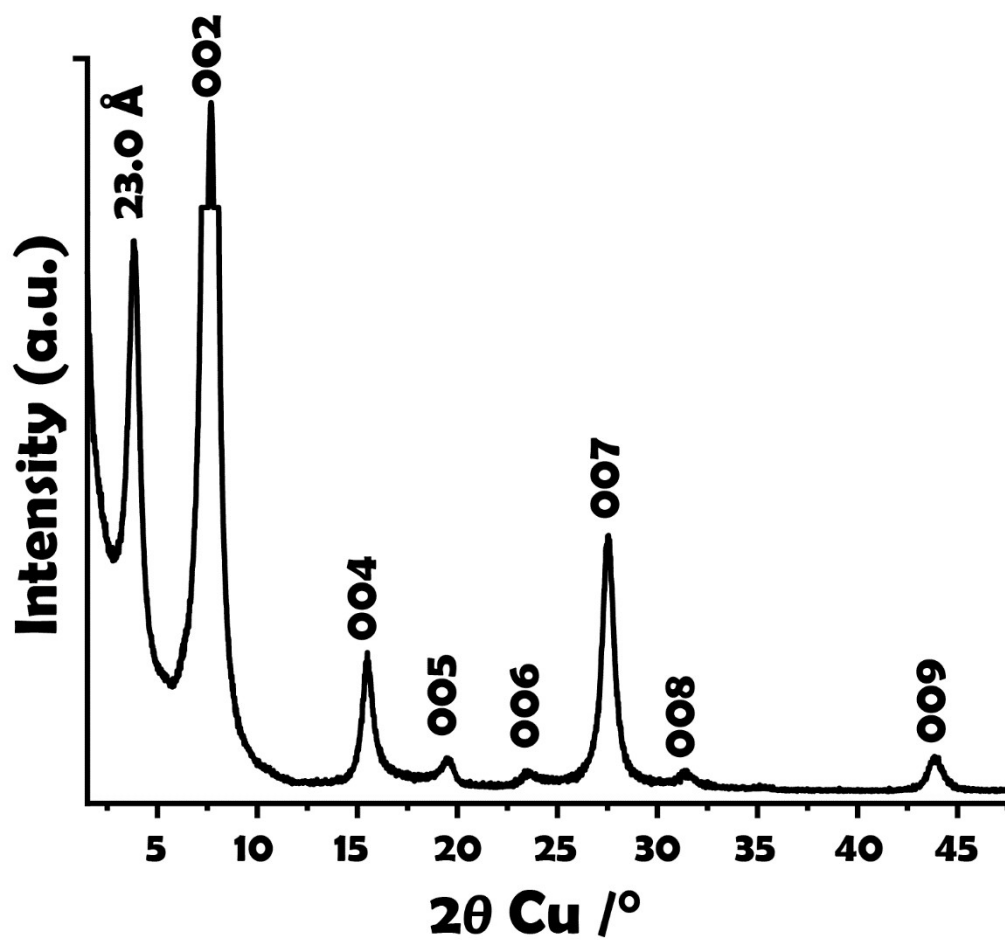


Figure S4. PXRD of the ordered interstratification of strictly alternating Na^+ and NH_4^+ layers in synthetic hectorite. The sample was equilibrated in an atmosphere with 43% relative humidity.

ICP-OES

Table S1. Elemental composition according to ICP-OES.

Element	Weight fraction of the element [%]		
	5 wt%	30 wt%	60 wt%
Nominal Au			
Au	6	25	57
Mg	15.3	12.3	7
Nominal Formula ^a	$(\text{Au})_{0.12} \text{Li}_{0.31}(\text{Mg}_{2.5}\text{Li}_{0.5}\text{Si}_4\text{O}_{10}\text{F}_2)$	$(\text{Au})_{0.68} \text{Li}_{0.31}(\text{Mg}_{2.5}\text{Li}_{0.5}\text{Si}_4\text{O}_{10}\text{F}_2)$	$(\text{Au})_{2.5} \text{Li}_{0.31}(\text{Mg}_{2.5}\text{Li}_{0.5}\text{Si}_4\text{O}_{10}\text{F}_2)$

^aThe nominal formula was calculated to be $(\text{Au})_x \text{Li}_{0.31}(\text{Mg}_{2.5}\text{Li}_{0.5}\text{Si}_4\text{O}_{10}\text{F}_2)$. Si was not detected directly via ICP-AAS. The amount of Si was rather calculated assuming the atomic ratio of Mg to Si of 2.5:4 as required by the hectorite-composition.

SAXS modelling

To fit SAXS curves, a linear combination of a spherical model¹ (sphere) and lamellar stack² with appropriate weighted factors accounting for the varying volume ratios of the constituents (hectorite and Au NPs) was applied.

$$I(q) = \text{scale} * (A * \text{sphere} + B * \text{lammelar}) + \text{background}$$

Table S2. Model parameters of SAXS fitting

Parameter	AuDS 5	AuDS 30	AuDS 60	Physical meaning
Scale	0.003	0.0011	0.000878	Source intensity
Background	0.015	0.0044	0.01	Source background
A	0.002	0.026	0.0544	Weighted factor of nanoparticle
Scattering length density	$83.4 * 10^{-6} \text{ \AA}^{-2}$	$83.4 * 10^{-6} \text{ \AA}^{-2}$	$83.4 * 10^{-6} \text{ \AA}^{-2}$	nanoparticles scattering length density
Radius	35.8 \AA	35	38.5	Radius of nanoparticle
B	2.8	0.6933	1.1669	Weighted factor of nanosheets
Scattering length density	$22.2 * 10^{-6} \text{ \AA}^{-2}$	$22.2 * 10^{-6} \text{ \AA}^{-2}$	$22.2 * 10^{-6} \text{ \AA}^{-2}$	nanosheets scattering length density
Thickness	24.4 \AA	33	44.3	Thickness of nanosheet
Spacing	530 \AA	None	None	Separation between nanosheets

Please note that the contribution of the Au NPs to the total scattering increases due to the larger weighting factor of the spherical scatterer concomitantly with the increasing loading of Au NPs amounting to 0.7, 5.5 and 16.8 vol% for AuDS 5, AuDS 30 and AuDS 60 respectively. Additionally, the apparent thickness of the double stacks increases.

Top-view TEM images of AuDS

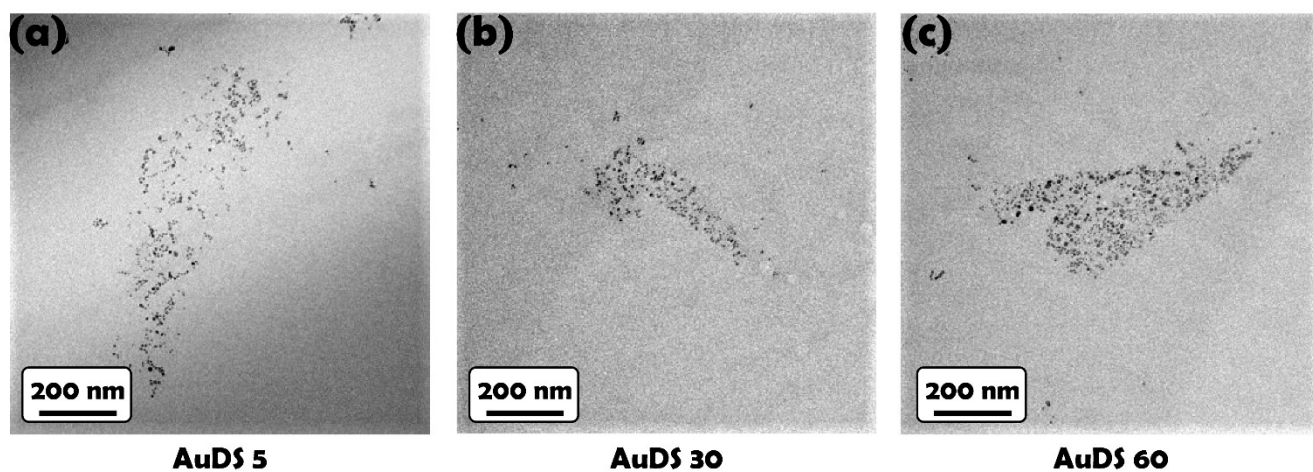


Figure S5. TEM images of AuDS with different Au NPs loading were used for determining the interparticle distance. **a** Top-view TEM image of AuDS 5. **b** Top-view TEM image of AuDS 30. **c** Top-view TEM image of AuDS 60

Patchy defogging pattern of glass coated with free Au NPs

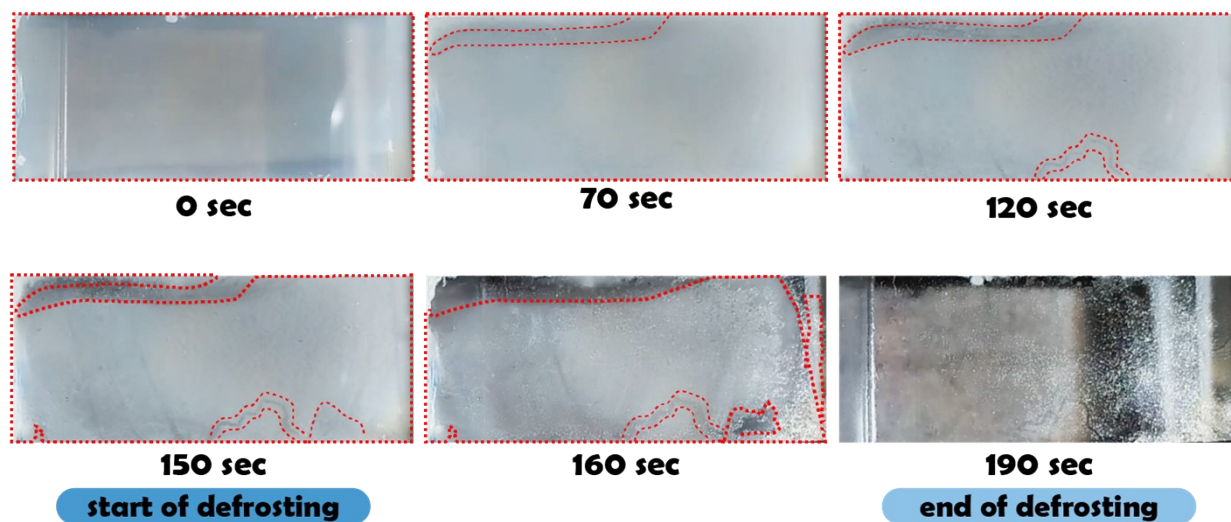


Figure S6. Sequence of images following the defrosting of a glass slide coated with DMAP capped Au NPs over time under 1 sun solar irradiation shows the patchy character of defogging pattern.

Photos of samples

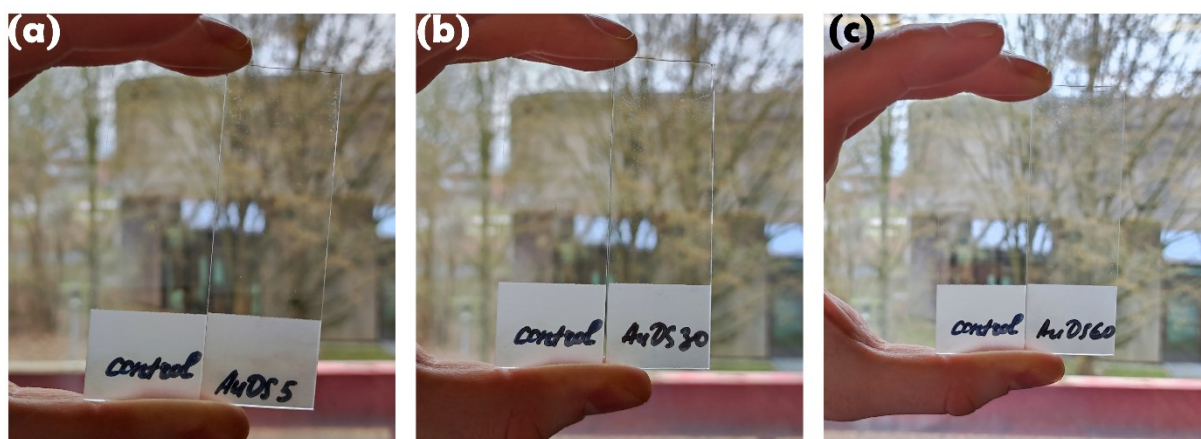


Figure S7. Comparison of transparency of an uncoated glass slide (left) and samples with applied metasurface (right) fabricated by dip coating showing the high transparency of the coating. **a** AuDS 5. **b** AuDS 30. **c** AuDS 60.

Defogging and defrosting tests

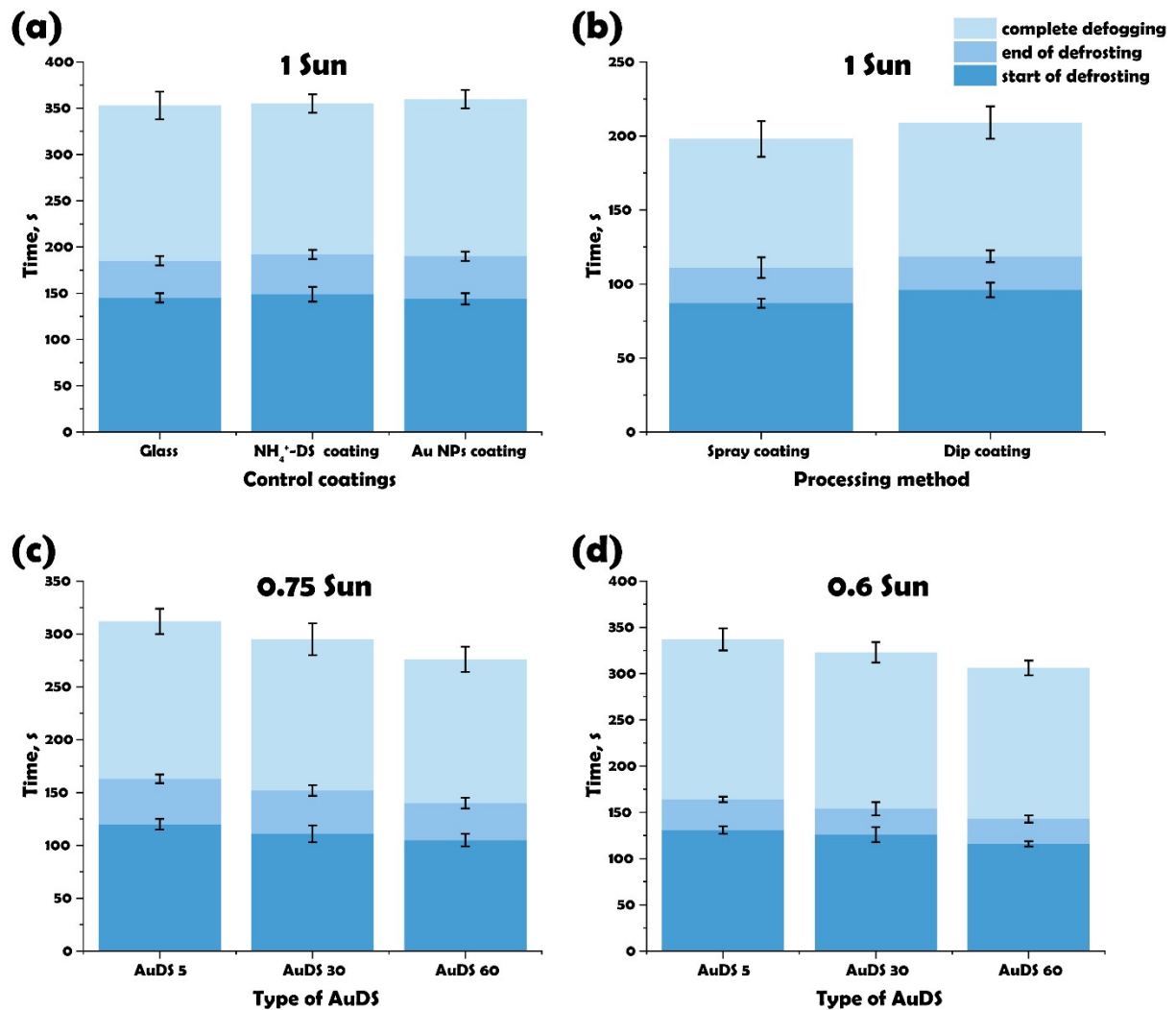
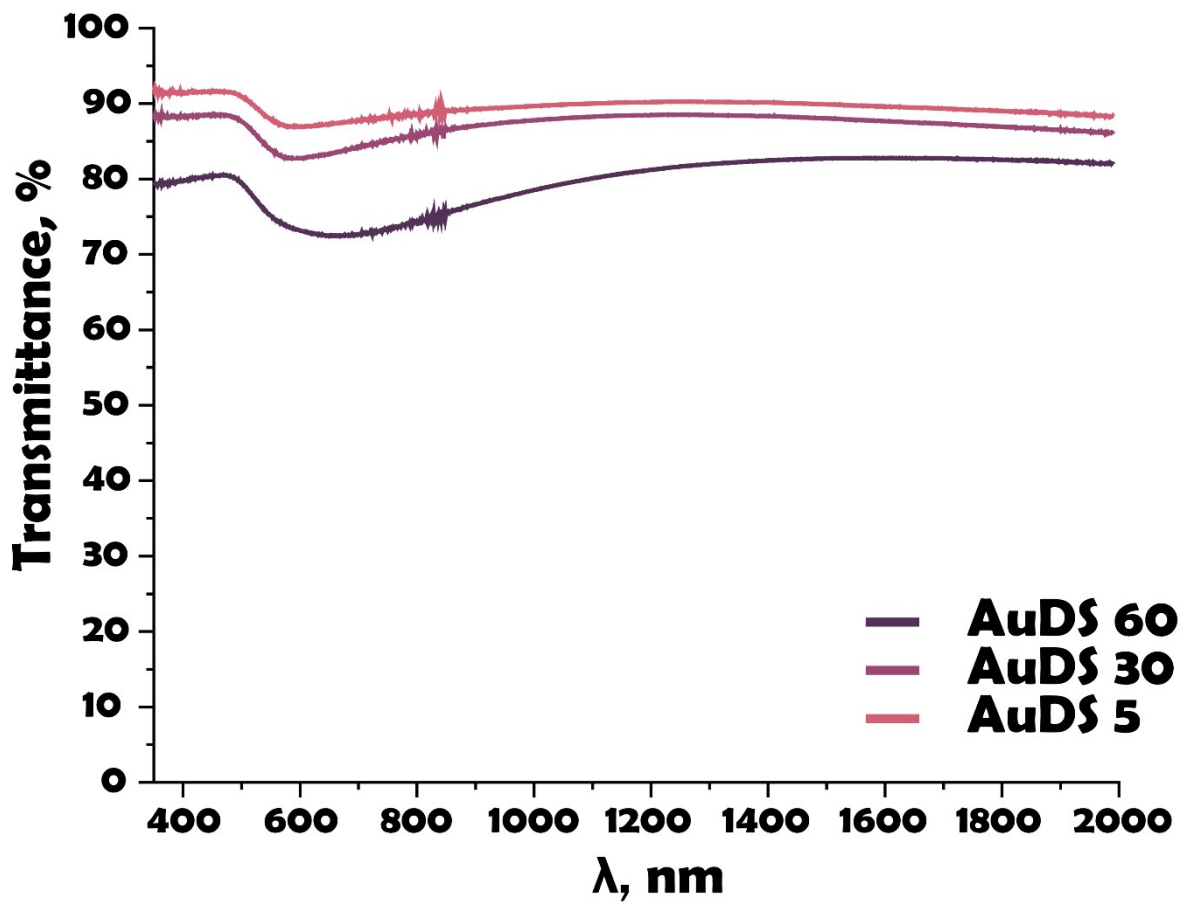
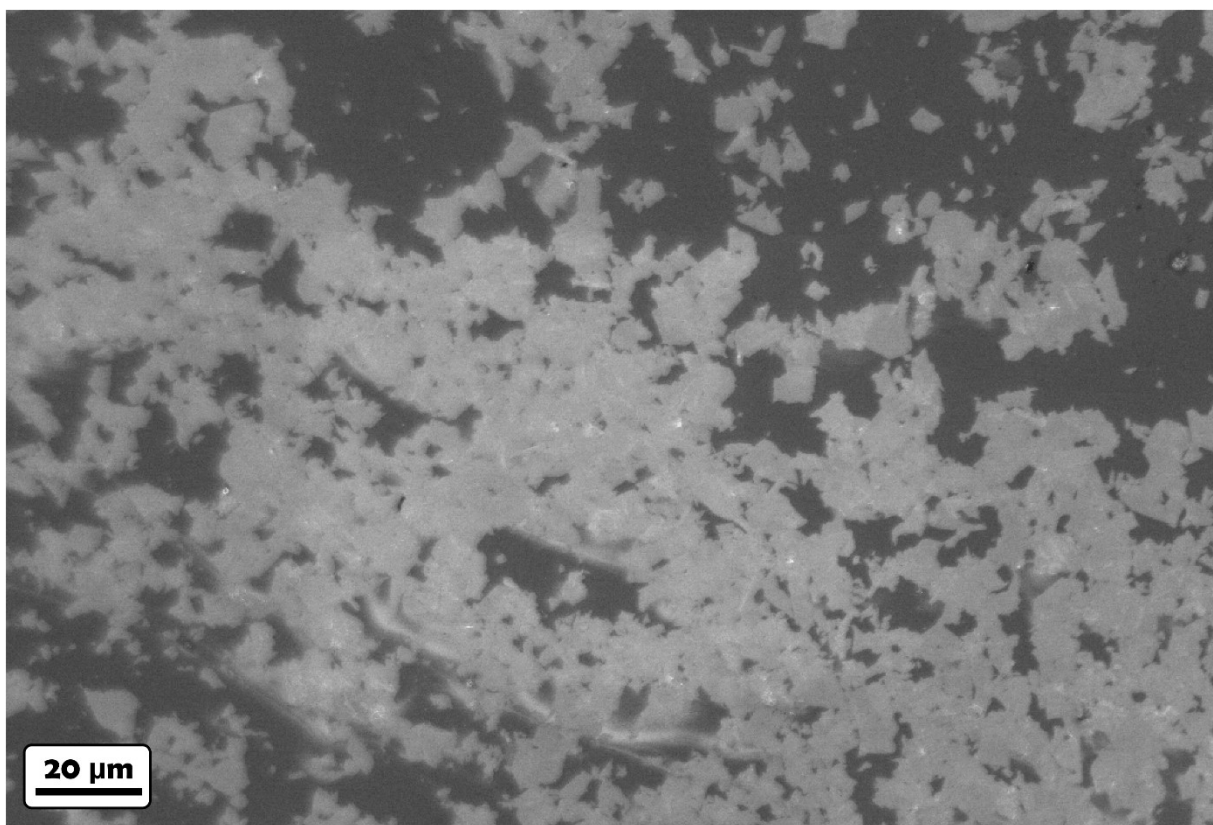


Figure S8. Defogging and defrosting tests. **a** Time dependency histogram of defogging for uncoated glass, glass coated with NH_4^+ -DS and glass coated with free DMAP capped Au NPs. **b** Time dependency histogram comparing different coating methods of AuDS 60 coated glass slides. **c** Time dependency histogram of defogging measured under 0.75 sun irradiation. **d** Time dependency histogram of defogging measured under 0.6 sun irradiation.



Transmission spectra of AuDS metasurfaces

Figure S9. Transmission spectra of AuDS coated metasurfaces.



SEM image of AuDS metasurface deposited via dip coating (3 layers)

Figure S10. SEM image of AuDS metasurface after 3 dip coating cycles showing increased coverage compared to 1 dip coating cycle.

SEM image of the AuDS metasurface deposited via spray coating

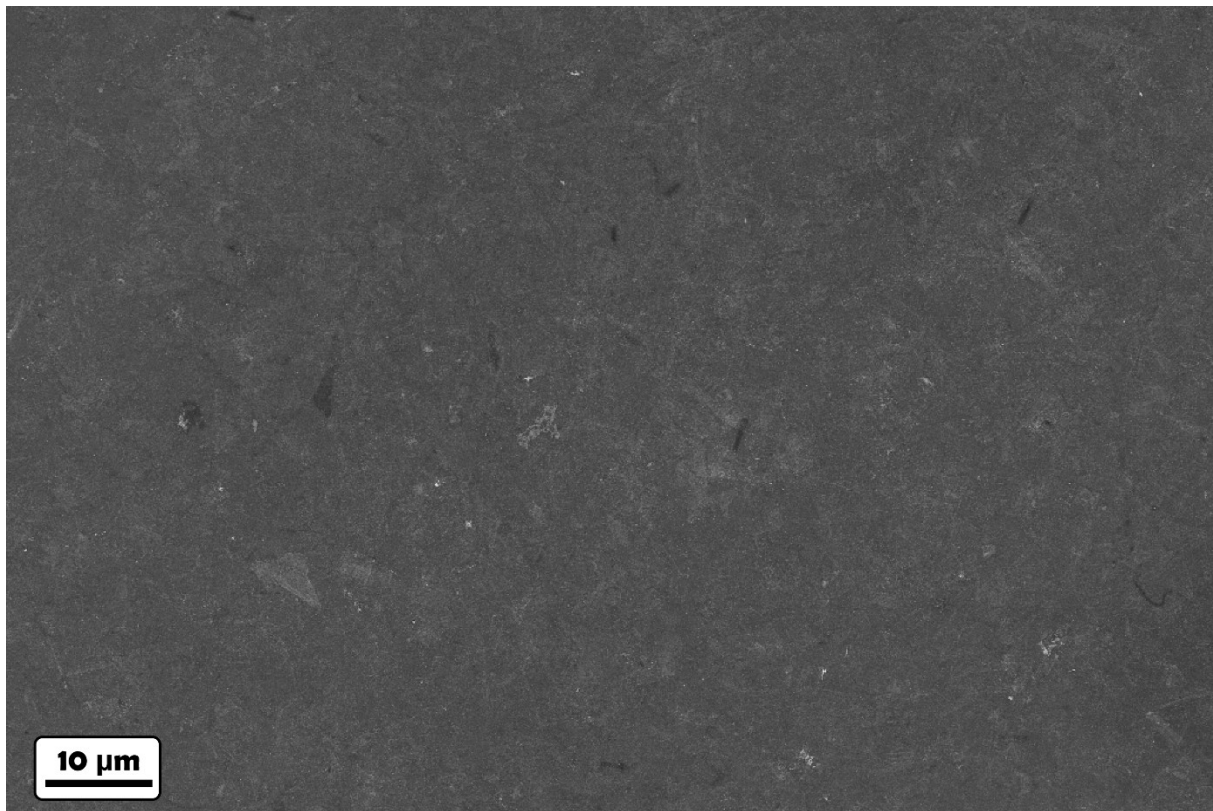


Figure S11. SEM image of AuDS metasurface deposited via spray coating showing full coverage.

Mean temperature increase

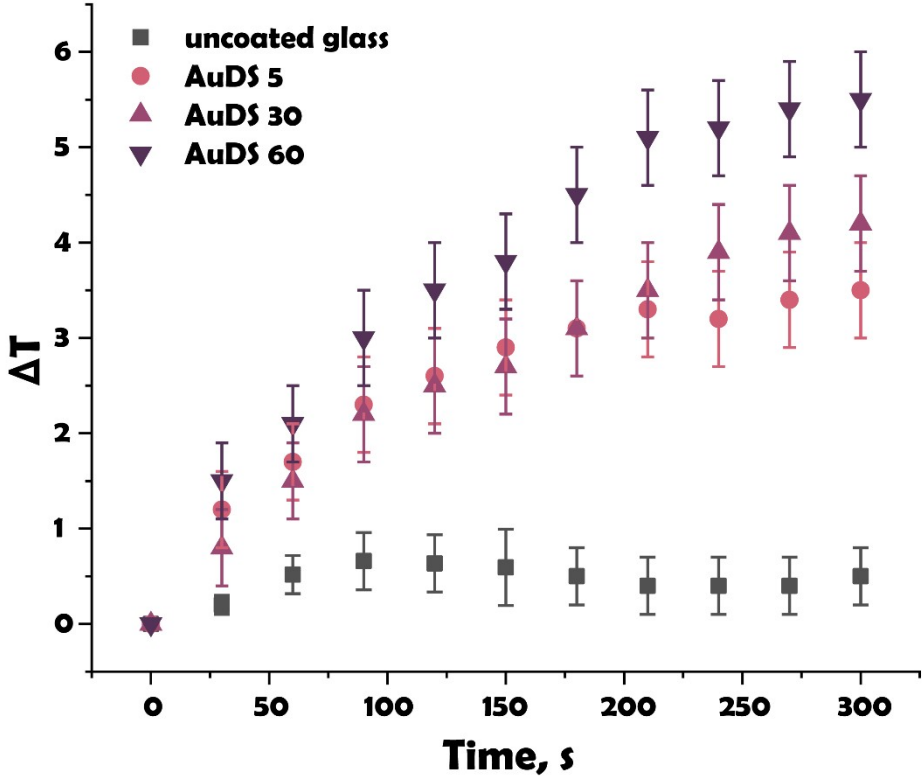


Figure S12. Mean temperature increase of the uncoated glass, glass coated with AuDS5, AuDS 30, and AuDS 60 metasurface under 1 sun illumination.

References:

1. A. Guinier, G. Fournet, C. B. Walker and G. Vineyard, *Phys. Today*, 1956.
2. F. Nallet, R. Laversanne and D. Roux, *J. Phys. II*, 1993, **3**, 487–502.